Original Article: Computational Chemistry Approach for the Investigation of Structural, Electronic, Chemical and Quantum Chemical Facets of Twelve Biginelli Adducts

Vishnu A. Adole (ORCID)

PG Department of Chemistry, Mahatma Gandhi Vidyamandir's Arts, Science and Commerce College, Manmad, Taluka-Nandgaon, District-Nashik, India-423104

ABSTRACT

The rising concerns about the Biginelli reaction are mainly attributed to the therapeutic and pharmacological features of Biginelli adducts, especially dihydropyrimidinones (DHPMs). The density functional theory (DFT) framework could be used to explore molecular properties such as molecular structures, molecular energies, ionisation potentials, dipole moments, and electronic parameters. It also contributes to the correlative analysis of theoretical and experimental findings through providing valuable perspectives. Using DFT method with the 6-311++G(d,p) basis set, twelve Biginelli adducts were focused to ascertain various structural and chemical parameters. The important structural parameters such as optimized molecular structures, frontier molecular orbital (FMO) analysis, and molecular electrostatic potential analysis are addressed in the present report. In addition, different quantum chemical parameters were calculated to gain a deeper comprehension of the molecules' synthetic reactivity. The FMO and quantum chemical exploration revealed that **BA7** molecule has a lower HOMO-LUMO energy gap, indicating that charge transfer interactions are inevitable within the molecule. The **BA7** molecule was also found to have a higher global softness value than the other derivatives. The absolute hardness of the **BA6** molecule, on the other hand, was higher. With a value of 2.2291 eV, the **BA3** molecule was revealed to have the highest charge transfer.

Introduction

The therapeutic and pharmacological properties of Biginelli adducts, specifically DHPMs, have sparked increased interest in the Biginelli reaction [1]. Antimalarial, antileishmanial, antitubercular, antioxidant, antidiabetic, antiproliferative, anticancer effects, calcium channel inhibition, anti-inflammatory, antihypertensive, etc., have all been observed in various DHPMs and related compounds [2]. Conversely, in the following years, this reaction was largely ignored, and

---

*Corresponding Author: Vishnu A. Adole (vishnuadole86@gmail.com)

thus the synthetic attributes of dihydropyrimidinones remained unknown until the 1970s. Interest grew rapidly in the 1970s, and since late 1980, an unprecedented boom has emerged as a result of a rise in the number of publications and patents. Numerous studies on the synthesis and chemical properties of Biginelli adducts have been published since then. For the synthesis of DHPMs, their thione analogues, and their heterocyclic derivative compounds, a broad range of reaction modifications have been produced. There have been reports of Biginelli adducts with high pharmacological potential. Monastrol (**a**) and its derivative piperastrol (**b**) have been reported as powerful anticancer agents in Biginelli adducts, which are promising compounds for the treatment of cancers (**Fig. 1**). **Figure 1** also shows other anticancer Biginelli adducts such as [R]-(+)-Mon-97 (**c**) and [R]-Fluorastro (**d**). **Figure 2** depicts the Biginelli adducts with potent antitubercular activity (**e** and **f**). **Figure 3** shows the Biginelli adducts, which have a strong antimalarial effect (**g** and **h**).
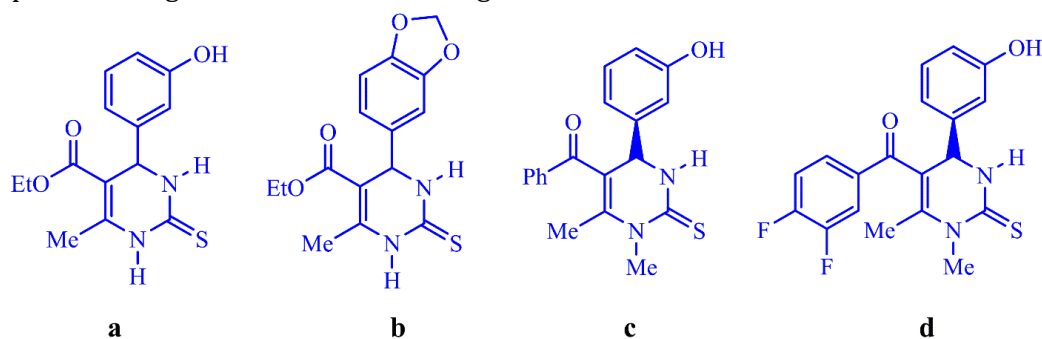
Figure 1. Biginelli adducts having anticancer activity
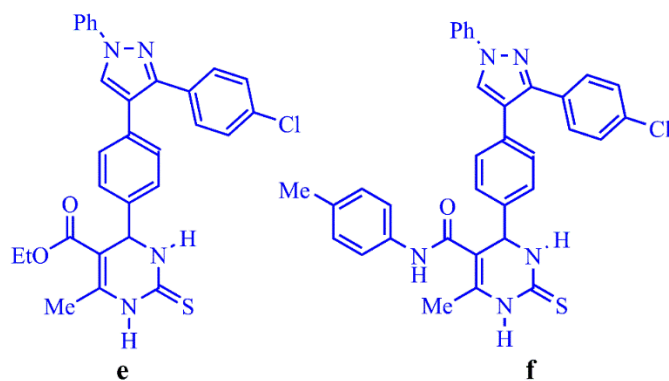
Figure 2. Biginelli adducts having antitubercular activity
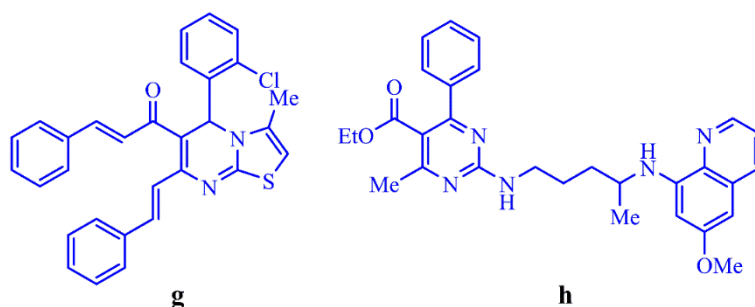
Figure 3. Biginelli adducts having antimalarial activity

Quantum chemical method allows the prediction of different properties based on knowledge of a few quantum superposition and the use of standard programming for electronic structure calculations [3-16]. DFT has gained a lot of attention in the last two decades because it is less computationally expensive. B3LYP stands for "Becke, 3-parameter, Lee-Yang-Parr". The DFT based on theoretical quantum calculations has been effectively used to explore the structural and chemical properties of organic molecules [17-22] The importance of spectroscopic and quantum calculations in predicting various quantum chemical parameters and thermodynamic aspects has been discovered [23-25]. Various structural and quantum chemical parameters of twelve Biginelli adducts were investigated in the light of the aforementioned essential aspects in the current analysis.

Computational details

The well-known DFT method through the B3LYP method was used for calculations [26]. The detailed about this function and its advantage was described in the literature [26, 27]. DFT simulations were performed using the Gaussian-03 programme package on an Intel (R) Core (TM) i5 computer with no geometry constraints [28]. The DFT/B3LYP method was used to investigate structural elements such as optimized molecular geometry, bond length, atomic charges, and bon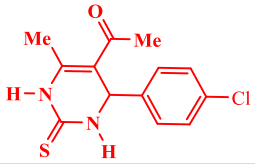d angle of previously synthesi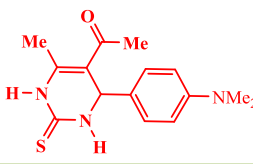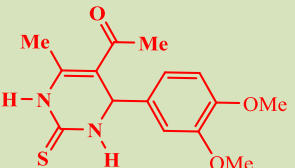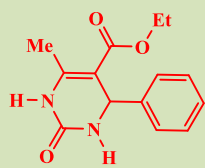zed Biginelli adducts [29] using the 6-311++G(d,p) basis set. The Gauss View 4.1.2 molecular visualisation programme was used to establish optimized geometry. Some quantum-chemical calculations were performed using the DFT method with the same basis set for a detailed molecular structure explanation. All of the calculations were done in the gas phase for the optimized structure. The quantum and structural entities such as total energy, electron density distribution in highest occupied molecular orbital (HOMO) and lowest unoccupied molecular orbital (LUMO), charge distribution, electronegativity (χ), absolute hardness (η), softness (σ), electrophilicity (ω), chemical potential (Pi), charge transfer in molecules (ΔN_{max}) have been computed. Theoretical investigations were also used to investigate the molecular electrostatic potential (MEP).

Results and discussion

Molecular structure study

The twelve Biginelli adducts that were previously synthesised have been labelled **BA1** to **BA12**. **Table 1** shows the structures of the previously synthesised Biginelli adducts. **Figure 4** shows the optimized molecular structure of Biginelli adducts. As predicted by DFT study, all Biginelli adducts have C1 point group symmetry. Of all Biginelli adducts, the molecule **BA4** has the highest polarity (μ = 5.2956 Debye), whereas the molecule **BA6** has the lowest one (μ = 3.4750 Debye).
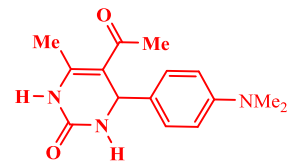
Table 1. Structures of the Biginelli adducts and their abbreviations used

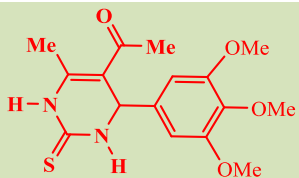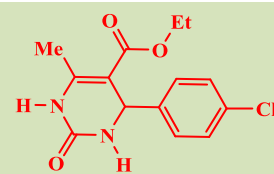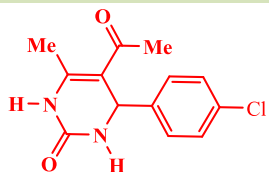| Entry	Biginelli adduct	Entry	Biginelli adduct
BA1		**BA7**	
BA2		**BA8**	

BA3
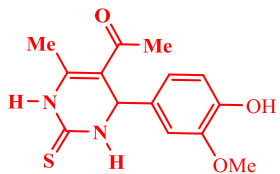
BA9

BA4

BA10

BA5

BA11

BA6

BA12

BA1

BA2

BA3

BA4

BA5

BA6

BA7

BA8

BA9

BA10

BA11
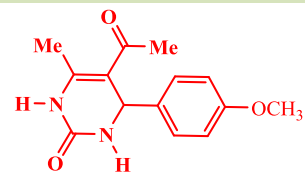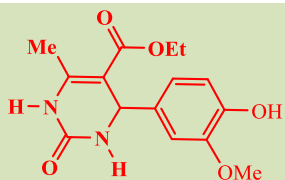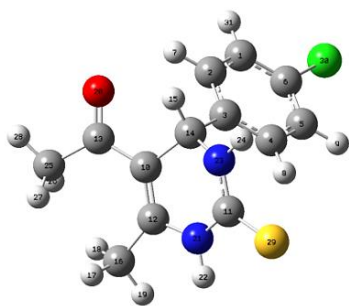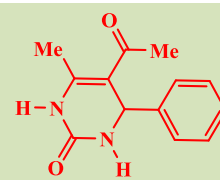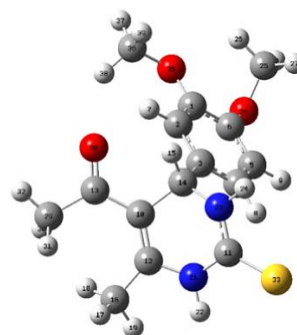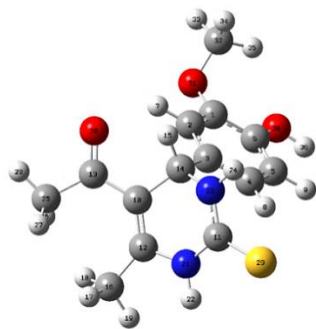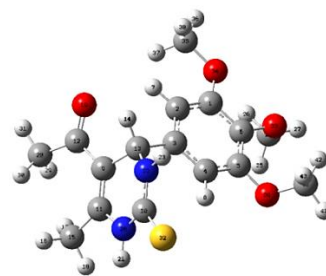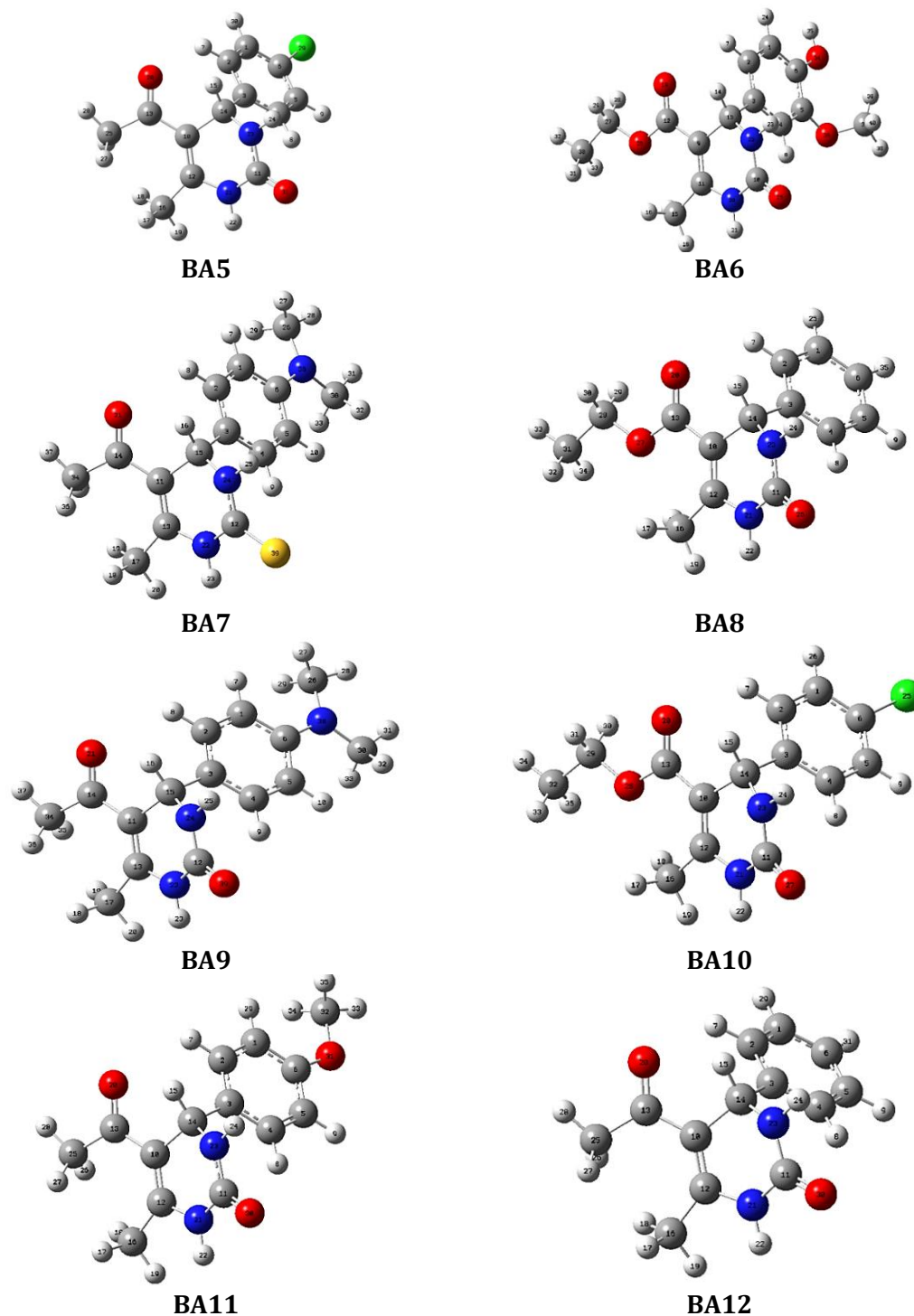
BA12

Figure 4. Optimized molecular structures of Biginelli adducts (BA1 to BA12)

Frontier molecular orbital study

The FMOs; HOMO and LUMO, are critical for determining a molecule's reactivity and stability. E_{HOMO} and E_{LUMO} are both associated with electron-donating and electron-accepting potential. The narrower the energy difference between HOMO and LUMO, the more stable a molecule becomes. As a result, it is clear that the HOMO-LUMO energy gap is a significant indicator of unsaturated systems' kinetic stability. The HOMO-LUMO energy gap is

expanded, which reduces a molecule's stability, polarizability, and electron transport. E_{HOMO} and E_{LUMO} values are crucial since they reflect ionisation enthalpy and electron affinity, respectively. The nucleophilic power of a compound is determined by its E_{HOMO} value, while its electrophilic character is determined by its E_{LUMO} value. The chemical reactivity switches with the molecular arrangement of the molecule, as shown by these two parameters. The wave function research demonstrates that electron absorption corresponds to the transition from the ground state to the first excited state, which is primarily represented by a single electron transition from the highest occupied to lowest unoccupied molecular orbital.

The global reactivity descriptors were calculated from molecular parameters a per previously reported methods [30, 31]. The ionization potential (I), electron affinity (A), band gap energy (E_g), electronegativity (χ), absolute hardness (η), global softness (σ), global electrophilicity (ω), chemical potential (Pi), and maximum number of electrons transferred (N_{max}) have all been determined using FMO's energies. With the support of the η and σ parameters, the donor-acceptor phenomenon of a chemical system can be easily predicted. A hard molecule has a large energy gap, whereas a soft molecule has a small energy gap. As a result, soft molecules may be more polarizable than hard molecules. The absolute hardness and global softness are related to the chemical structure's stability and correspond to the distance between the E_{HOMO} and E_{LUMO}. The chemical potential (Pi) of an electron determines its ionisation potential, which is also linked to its χ. The tendency of a molecule to lose an electron increases as the Pi value rises. Chemical hardness and chemical potential are important aspects of a molecule's overall reactivity and are important components of charge transfer. A lower value of ω indicates the strong nucleophilic nature, while higher values indicate strong electrophilic nature, The FMO of Biginelli adducts (**BA7** and **BA8**) are represented in **Figure 5**. **Table 2** shows the electronic parameters of Biginelli adducts, while **Table 3** shows global reactivity descriptors. According to the FMO examination, molecule **BA7** has the smallest energy difference, while molecule **BA8** has the largest. This knowledge is important for evaluating the molecule's reactivity and charge transfer phenomena.
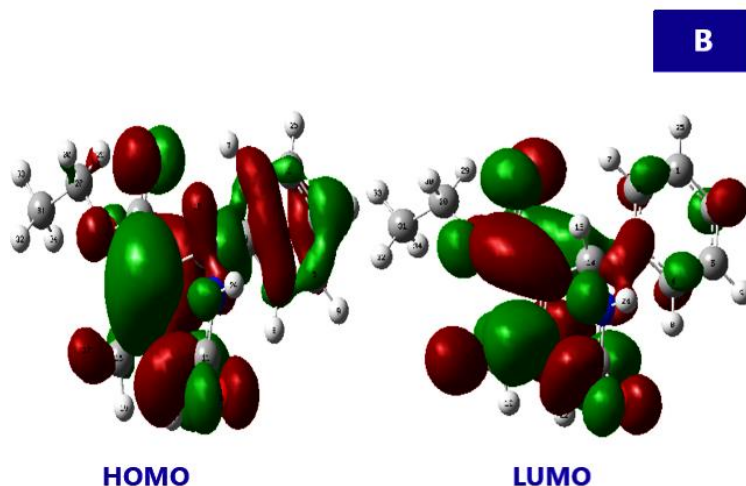

A

HOMO   **LUMO**
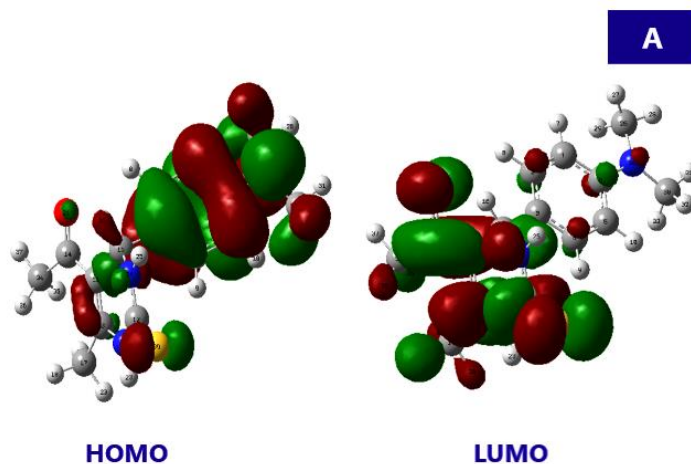
Figure 5. Frontier molecular orbital pictures; A: BA7 and B: BA8

Table 2. Electronic parameters of Biginelli adducts

Entry	E (a.u.)	E_{HOMO} (eV)	E_{LUMO} (eV)	I (eV)	A (eV)	E_g (eV)
BA1	−1546.5798	−6.2790	−2.2637	6.2790	2.2637	4.01
BA2	−1316.0384	−6.0430	−2.2808	6.0430	2.2808	3.76
BA3	−1276.7394	−6.1287	−2.3228	6.1287	2.3228	3.79
BA4	−1430.6071	−6.0275	−2.2884	6.0275	2.2884	3.80
BA5	−1223.6237	−6.7170	−1.9456	6.7170	1.9456	3.74
BA6	−1068.3156	−7.5393	−2.0993	7.5393	2.0993	4.77
BA7	−1220.9604	−5.3935	−1.9505	5.3935	1.9505	3.44
BA8	−878.5878	−6.5211	−1.4824	6.5211	1.4824	5.04
BA9	−898.0018	−5.3445	−1.6863	5.3445	1.6863	3.66
BA10	−1338.1575	−6.8125	−2.1900	6.8125	2.1900	4.62
BA11	−878.5110	−6.6920	−2.1377	6.6920	2.1377	4.55
BA12	−763.9212	−6.7369	−2.1423	6.7369	2.1423	4.59

Note: Abbreviations: I, ionization potential; A, electron affinity; Note: I = −E_{HOMO} & A = −E_{LUMO}.

In comparison to the other Biginelli adducts, the molecule **BA7** has a lower HOMO-LUMO energy gap, indicating that charge transfer interactions are unavoidable within the molecule. **BA7** has the most reactive HOMO (E_{HOMO} = −5.3445 eV) and **BA6** has the least reactive HOMO (E_{HOMO} = −7.5393 eV) of all Biginelli adducts. In molecule **BA3** (E_{LUMO} = −2.3228 eV), the LUMO has a lower energy and with high energy in the molecule **BA8** (E_{LUMO} = −1.4824 eV). **BA6** has the highest ionization potential (I = 7.5393 eV), while **BA7** (I = 5.3445 eV) has the lowest. The molecule **BA3** has a higher electron affinity value (A = 2.3228 eV) than the molecule **BA8** (A = 1.4824 eV). Since the global electrophilicity value is greater than 1.5 eV, the global descriptor study indicates that all Biginelli adducts would be strong electrophiles. When it comes to global softness, the molecule **BA7** has a higher value than the other derivatives, with a global softness value of 0.5809 eV. The absolute hardness of the molecule **BA6** is higher, which is 2.7200 eV. **BA3** is the molecule with the highest charge transfer, with a value of 2.2291 eV.

Table 3. Global reactivity parameters of Biginelli adducts

Entry	X (eV)	η (eV)	σ (eV⁻¹)	ω (eV)	Pi(eV)	ΔN_{max} (eV)	μ (Debye)
BA1	4.2713	2.0076	0.4981	4.5437	−4.2713	2.1275	4.8199
BA2	4.1619	1.8811	0.5316	4.6041	−4.1619	2.2125	3.7383

BA3	4.2308	1.8980	0.5269	4.7154	−4.2308	2.2291	4.2775
BA4	4.1580	1.8695	0.5349	4.6238	−4.1580	2.2241	5.2956
BA5	4.3313	2.3857	0.4192	3.9318	−4.3313	1.8155	4.5894
BA6	4.8193	2.7200	0.3676	4.2694	−4.8193	1.7718	3.4750
BA7	3.6720	1.7215	0.5809	3.9162	−3.6720	2.1330	5.1408
BA8	4.0018	2.5193	0.3970	3.1783	−4.0018	1.5884	3.9845
BA9	3.5154	1.8291	0.5467	3.3782	−3.5154	2.1503	4.6953
BA10	4.5012	2.3113	0.4326	4.3831	−4.5012	1.9475	4.8463
BA11	4.4148	2.2771	0.4391	4.2796	−4.4148	1.9387	3.5945
BA12	4.4396	2.2973	0.4353	4.2899	−4.4396	1.9326	4.8359

Note: $\chi = (I + A)/2$; $\eta = (I - A)/2$; $\sigma = 1/\eta$; $\omega = Pi^2/2\eta$; $Pi = -\chi$; $\Delta N_{max} = -Pi/\eta$. Abbreviations: χ, electronegativity; η, absolute hardness; σ, global softness; ω, global electrophilicity; Pi, chemical potential; ΔN_{max}, maximum no. of electron transferred.

Molecular electrostatic plot study

The red and yellow regions on the pyrimidinone/thione nucleus, according to these MEP plots (Figure 6), show a region of high electron density. The green zone is often found on the saturated portion and represents zero potential regions. The blue part, on the other hand, represents nucleophilic reactivity. The molecular electrostatic potential (MEP) can be used to correlate properties such as dipole moment, electronegativity, partial charges, and chemical reactivity of any molecule. The use of a MEP can be used to evaluate phenomena such as nucleophilic and electrophilic locations, solvent effects, hydrogen bonding interactions, and so on. The MEP has emerged as a convincing guide to look at molecular interactions in recent years. It has been successfully linked to a wide range of biological and chemical scaffolds in modern science. The total charge distribution of a molecule space is the MEP. The various electrostatic potential values at the molecule's surface are expressed by different colours. Positive, negative, and neutral potentials are all represented by different colours. Electrophilic reactivity is correlated with the red and yellow zones, which leads to high electron density. Low electron density and nucleophilic reactivity are expressed by the blue parts, while positive electrostatic potential is represented by the white parts. Green colours, on the other hand, reflect areas with no potential. These zones of varying electrostatic potential may provide useful information about different forms of intermolecular interactions, allowing one to predict a molecule's chemical behaviour. The electrophilic and nucleophilic sites indicate the area of the compound where it can interact.
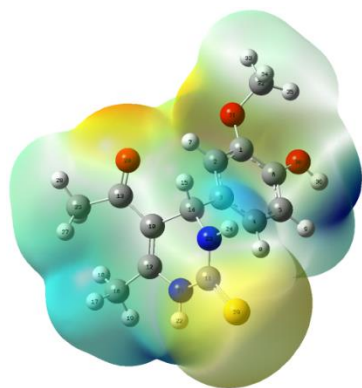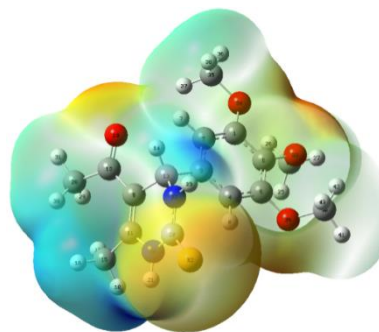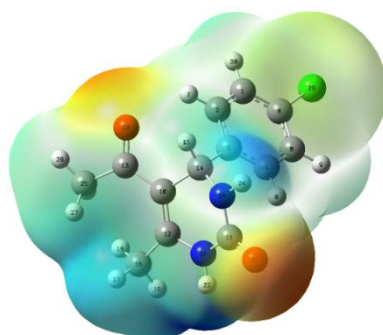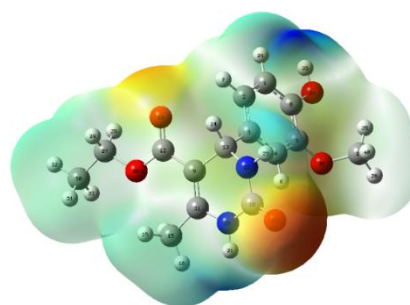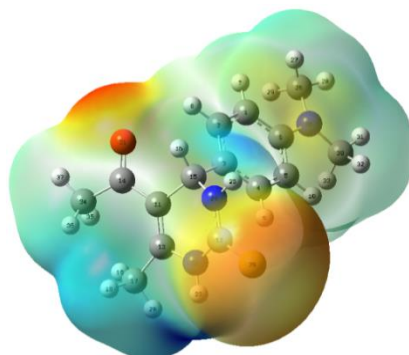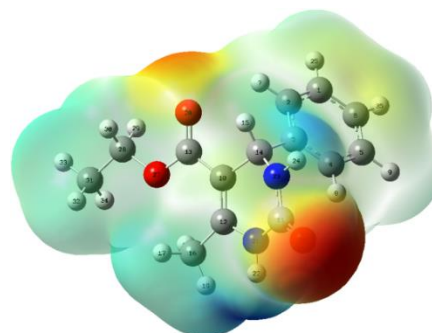

BA1

BA2

BA3
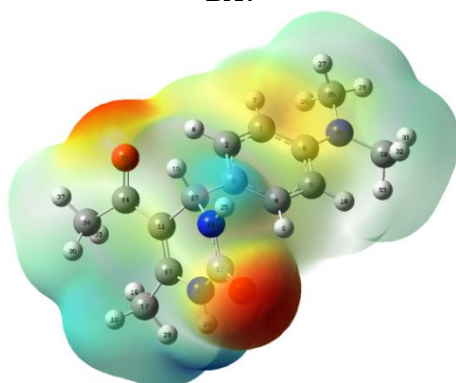
BA4

BA5

BA6
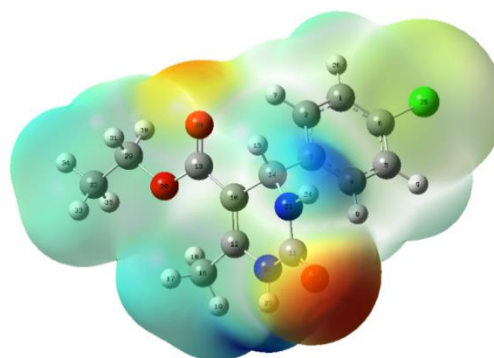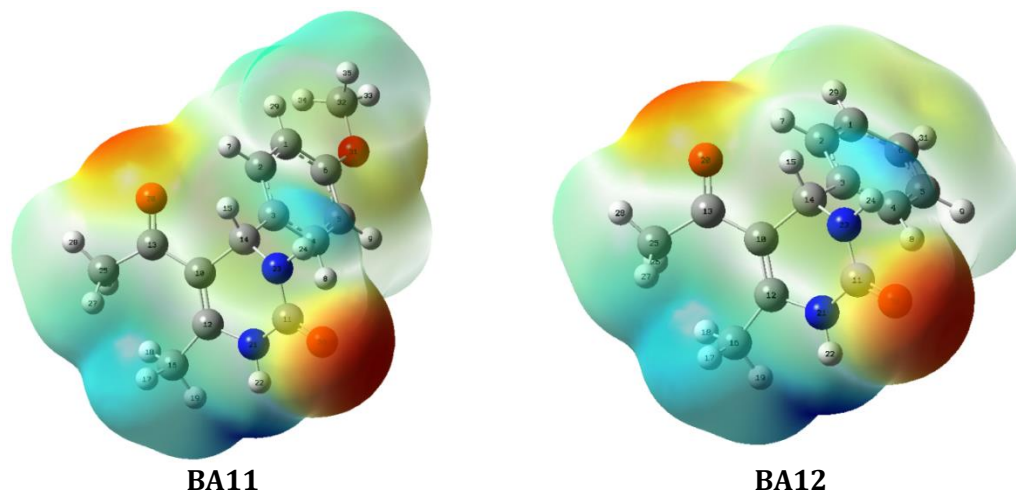
BA7

BA8

BA9

BA10

BA11   **BA12**
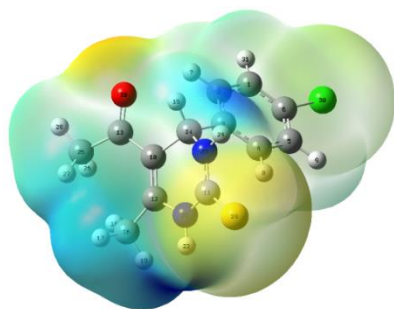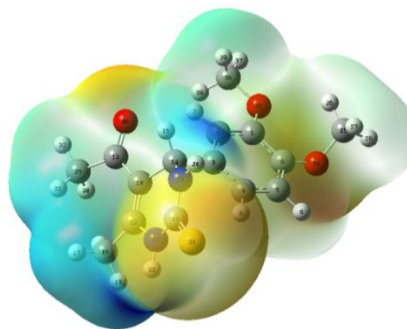
Figure 6. MEP plots for the Biginelli adducts

Conclusion

In conclusion, twelve Biginelli adducts were investigated structurally using the DFT approach with the 6-311++G(d,p) basis set. To examine the stability and chemical behaviour, structural parameters such as molecular descriptors and global reactivity descriptors were addressed. The negative potential sites were found around oxygen atoms, while the positive potential sites were found around hydrogen atoms, according to the MEP map. Total energy, electron density distribution in the HOMO and LUMO, charge distribution, electronegativity, absolute hardness, softness, electrophilicity, chemical potential, and charge transfer in molecules were measured. All Biginelli adducts were found to have C1 point group symmetry. The molecule **BA4** was the most polar amongst studied Biginelli adducts. The **BA7** molecule was shown to have a narrower HOMO-LUMO energy gap, implying that charge transfer interactions would occur within the molecule. The global softness value of the **BA7** molecule was also found to be higher than that of the other derivatives. The **BA6** molecule, on the other hand, possesses higher absolute hardness The **BA3** molecule was revealed to have the largest charge transfer. The current quantum chemical analysis could contribute to a better understanding of the properties of the title molecules, as well as its application in more advanced applications.

Conflict of interest

Author does not have any conflicting interest.

Orcid

Vishnu A. Adole: https://www.orcid.org/0000-0001-7691-7884

References

[1] a) C.O. Kappe, *Eur. J. Med. Chem.*, **2000**, *35*, 1043-1052. **[crossref], [Google Scholar] , [Publisher]**
b) Â. de Fátima, T.C. Braga, L.S. Neto, B.S. Terra, B.G.F. Oliveira, D.L. da Silva, L.V. Modolo, *J. Adv. Res.*, **2015**, *6*, 363-373. **[crossref], [Google Scholar] , [Publisher]**
[2] a) K. Singh, T. Kaur, *MedChemComm*, **2016**, *7*, 749-768. **[Crossref], [Google Scholar], [Publisher]** b) U. Rashid, R. Sultana, N. Shaheen, S.F. Hassan, F. Yaqoob, M.J. Ahmad, F. Iftikhar, N. Sultana, S. Asghar, M. Yasinzai, F.L. Ansari, *Eur. J. Med. Chem.*, **2016**, *115*, 230-244.

[Crossref], **[Google Scholar]**, **[Publisher]** c) A.R. Trivedi, V.R. Bhuva, B.H. Dholariya, D.K. Dodiya, V.B. Kataria, V.H. Shah, *Bioorg. Med. Chem. Lett.*, **2010**, *20*, 6100-6102. **[Crossref]**, **[Google Scholar]**, **[Publisher]** d) A. de Vasconcelos, P.S. Oliveira, M. Ritter, R.A. Freitag, R.L. Romano, F.H. Quina, L. Pizzuti, C.M. Pereira, F.M. Stefanello, A.G. Barschak, *J. Biochem. Mol. ToxicoL.* **2012**, *26*, 155-161. **[Crossref]**, **[Google Scholar]**, **[Publisher]** e) K.L. Dhumaskar, S.N. Meena, S.C. Ghadi, S.G. Tilve, *Bioorg. Med. Chem, Lett.*, **2014**, *24*, 2897-2899. **[Crossref]**, **[Google Scholar]**, **[Publisher]** f) F.S. De Oliveira, P.M. De Oliveira, L.M. Farias, R.C. Brinkerhoff, R.C.M. Sobrinho, T.M. Treptow, C.R.M. D'Oca, M.A. Marinho, M.A. Hort, A.P. Horn, D. Russowsky, *MedChemComm*, **2018**, *9*, 1282-1288. **[Crossref]**, **[Google Scholar]**, **[Publisher]** g) C.M. Wright, R.J. Chovatiya, N.E. Jameson, D.M. Turner, G. Zhu, S. Werner, D.M. Huryn, J.M. Pipas, B.W. Day, P. Wipf, J.L. Brodsky, *Bioorg. Med. Chem.*, **2008**, *16*, 3291-3301. **[Crossref]**, **[Google Scholar]**, **[Publisher]** h) B.P. Kumar, G. Sankar, R.N. Baig, S. Chandrashekaran, *Eur. J. Med. Chem.*, **2009**, *44*, 4192-4198. **[Crossref]**, **[Google Scholar]**, **[Publisher]** i) K.S. Atwal, G.C. Rovnyak, J. Schwartz, S. Moreland, A. Hedberg, J.Z. Gougoutas, M.F. Malley, D.M., Floyd, *J. Med. Chem.*, **1990**, *33*, 1510-1515. **[Crossref]**, **[Google Scholar]**, **[Publisher]** j) P. Sharma, N. Rane, V. K. Gurram, *Bioorg. Med. Chem. Lett.*, **2004**, *14*, 4185-4190. **[Crossref]**, **[Google Scholar]**, **[Publisher]** k) S.N. Mokale, S.S. Shinde, R.D. Elgire, J.N. Sangshetti, D.B. Shinde, Bioorg. Med. Chem. Lett., **2010**, *20*, 4424-4426. **[Crossref]**, **[Google Scholar]**, **[Publisher]** l) A.M. Farghaly, O.M. AboulWafa, Y.A. Elshaier, W.A. Badawi, H.H. Haridy, H.A. Mubarak, *Med. Chem, Res.*, **2019**, *28*, 360-379. **[Crossref]**, **[Google Scholar]**, **[Publisher]** m) V.A. Adole, *World J. Pharm. Res.*, **2020**, *9*, 1067-1091. **[Crossref]**, **[Google Scholar]**, **[Publisher]**

[3] V.A. Adole, R.H. Waghchaure, S.S. Pathade, M.R. Patil, T.B. Pawar, B.S. Jagdale, *Mol. Simul.*, **2020**, *46*, 1045-1054. **[Crossref]**, **[Google Scholar]**, **[Publisher]**

[4] V.A. Adole, T.B. Pawar, B.S. Jagdale, *J. Sulphur Chem.*, **2021**, *42*, 131-148. **[Crossref]**, **[Google Scholar]**, **[Publisher]**

[5] V.A. Adole, B.S. Jagdale, T.B. Pawar, B.S. Desale, *Mat. Sci. Res. India*, **2020**, 17(specialissue2020), 13-36. **[Crossref]**, **[Google Scholar]**, **[Publisher]**

[6] T.B. Pawar, B.S. Jagdale, A.B. Sawant, V.A. Adole, *J. Chem. Biol. Phys. Sci.*, **2017**, *7*, 167-175. **[Pdf]**, **[Google Scholar]**, **[Publisher]**

[7] R.A. Shinde, V.A. Adole, B.S. Jagdale, T.B. Pawar, B.S. Desale, R.S. Shinde, *Mat. Sci. Res. India*, **2020**, *17*(specialissue2020), 146-161. **[Pdf]**, **[Google Scholar]**, **[Publisher]**

[8] (a) R.A. Shinde, V.A. Adole, B.S. Jagdale, T.B. Pawar, *Mat. Sci. Res. India*, **2020**, *17*(specialissue2020), 54-72. **[Crossref]**, **[Google Scholar]**, **[Publisher]**; (b) S.V. GAIKWAD, M.V Gaikwad, P.D. Lokhande, *J. Appl. Organomet. Chem.*, 2021, *1*, 1-8. **[crossref]**, **[Pdf]**, **[Google Scholar]**, **[Publisher]**; (c) B.S. Hote, D.B. Muley, G.G. Mandawad, *J. Appl. Organomet. Chem.*, 2021, *1*, 9-16. **[crossref]**, **[Pdf]**, **[Google Scholar]**, **[Publisher]**

[9] K.S. Devi, P. Subramani, N. Sundaraganesan, M.S. Boobalan, D. Tamilvendan, *J. Mol. Struct.*, **2020**, *1219*, 128604. **[Crossref]**, **[Google Scholar]**, **[Publisher]**

[10] V.A. Adole, P.B. Koli, R.A. Shinde, R.S. Shinde, *Mat. Sci. Res. India*, **2020,** *17*(specialissue2020), 41-53. **[Crossref]**, **[Google Scholar]**, **[Publisher]**

[11] P. Rajamani, V. Vijayakumar, P. Nagaraaj, N. Sundaraganesan, *Polycyl. Aromat. Comp.*, **2020**, 1-21. **[Crossref]**, **[Google Scholar]**, **[Publisher]**

[12] S.S. Pathade, V.A. Adole, B.S. Jagdale, T.B. Pawar, *Mat. Sci. Res. India*, **2020**, *17*(special issue2020), 27-40. **[Crossref]**, **[Google Scholar]**, **[Publisher]**

[13] V.A. Adole, R.H. Waghchaure, B.S. Jagdale, T.B. Pawar, S.S. Pathade, J. Adv. Sci. Res., **2020**, *11*, 64-70. **[Crossref]**, **[Google Scholar]**, **[Publisher]**

[14] R.H. Waghchaure, T.B. Pawar, World *J. Pharm. Res.*, **2020**, *9*, pp.1867-1881. **[Crossref]**, **[Google Scholar]**, **[Publisher]** http://dx.doi.org/10.20959/wjpr20206-17663

[15] N. Karthikeyan, J.J. Prince, S. Ramalingam, S. Periandy, *Spectrochim. Acta A Mol. Biomol. Spectrosc.,* **2015**, *139*, 229-242. **[Crossref]**, **[Google Scholar]**, **[Publisher]**

[16] D.M. Gil, M.D. Lestard, O., Duque, J. Estévez-Hernández, E. Reguera, *Spectrochim. Acta A Mol. Biomol. Spectrosc.,* **2015**, *145*, 553-562. **[Crossref], [Google Scholar], [Publisher]**

[17] B.S. Jagdale, S.S. Pathade, *J. Appl. Chem.*, **2019**, *8*, 12-19. **[Pdf], [Google Scholar], [Publisher]**

[18] S.S. Pathade, B.S. Jagdale, *J. Adv. Sci. Res.*, **2020**, *11*, 87-94. **[Pdf], [Google Scholar], [Publisher]**

[19] S.L. Dhonnar, V.A. Adole, N.V. Sadgir, B.S. Jagdale, *Phys. Chem. Res.*, **2021**, *9*, 193-209. **[Crossref], [Google Scholar], [Publisher]**

[20] S.S. Pathade, B.S. Jagdale, *Phys. Chem. Res.*, **2020**, *8*, 671-687. **[Crossref], [Google Scholar], [Publisher]**

[21] E. Fereyduni, E. Vessally, E. Yaaghubi, N. Sundaraganesan, *Spectrochim. Acta A Mol. Biomol. Spectrosc.,* **2011**, *81*, 64-71. **[Crossref], [Google Scholar], [Publisher]**

[22] M. Shkir, S. AlFaify, H. Abbas, S. Muhammad, Spectrochim. *Acta A Mol. Biomol. Spectrosc.*, **2015**, *147*, 84-92. **[Crossref], [Google Scholar], [Publisher]**

[23] V.A. Adole, R.H. Waghchaure, B.S. Jagdale, T.B. Pawar, *Chem. Bio. Interface*, **2020**, *10*, 22-30. **[Pdf], [Google Scholar], [Publisher]**

[24] S.P. Vijaya Chamundeeswari, E. James Jebaseelan Samuel, N. Sundaraganesan, *Mol. Simul.*, **2012**, *38*, 987-1000. **[Crossref], [Google Scholar], [Publisher]**

[25] V.A. Adole, V. R. Bagul, S. A. Ahire, R. K. Pawar, G. B. Yelmame, A. R. Bukane, *J. Adv. Sci. Res.*, **2021**, *12*(1) Suppl 1, 276-286. **[Pdf], [Google Scholar], [Publisher]**

[26] a) A. D. Becke, *J. Chem. Phys.*, **1993**, *98*, 5648-5652. **[Crossref], [Google Scholar], [Publisher];** b) A.D. Becke, *J. Chem. Phys.*, **1993**, *98*, 1372-1377. **[Crossref], [Google Scholar], [Publisher]**

[27] S.A. Halim, M.A. Ibrahim, *J. Mol. Struct.*, *1130*, 543-558. **[Crossref], [Google Scholar], [Publisher]**

[28] M. J. Frisch, *et al.*, Gaussian 03 Revision E.01, Gaussian Inc., Wallingford CT. **2004**. **[Google Scholar], [Publisher]**

[29] V.A. Adole, T.B. Pawar, P.B. Koli, B.S. Jagdale, *J. Nanostructure Chem.*, **2019**, *9*, 61-76. **[Crossref], [Google Scholar], [Publisher]**

[31] V.A. Adole, B.S. Jagdale, T.B. Pawar, A.B. Sawant, *J. Chin. Chem. Soc.*, **2020**, *67*, 1763-1777. **[Crossref], [Google Scholar], [Publisher]**

[32] P. Rathi, R. Khanna, V.S. Jaswal, *J. Chin. Chem. Soc.*, **2020**, *67*, 213-217. **[Crossref], [Google Scholar], [Publisher]**